Electron spin resonance in a two-dimensional Fermi liquid with spin-orbit coupling

Saurabh Maiti,[1,2] Muhammad Imran,[1] and Dmitrii L. Maslov[1]
[1]*Department of Physics, University of Florida, Gainesville, Florida 32611, USA*
[2]*National High Magnetic Field Laboratory, Tallahassee, Florida 32310, USA*
(Received 9 October 2015; revised manuscript received 8 December 2015; published 26 January 2016)

Electron spin resonance (ESR) is usually viewed as a single-particle phenomenon protected from the effect of many-body correlations. We show that this is not the case in a two-dimensional Fermi liquid (FL) with spin-orbit coupling (SOC). Depending on whether the in-plane magnetic field is below or above some critical value, ESR in such a system probes up to three chiral-spin collective modes, augmented by the spin mode in the presence of the field, or the Silin-Leggett mode. All the modes are affected by both SOC and FL renormalizations. We argue that ESR can be used as a probe not only for SOC but also for many-body physics.

DOI: 10.1103/PhysRevB.93.045134

I. INTRODUCTION

Electron spin resonance (ESR) spectroscopy is an invaluable tool for studying dynamics of electron spins [1–3]. In a single-particle picture, ESR can be understood either classically, as resonant absorption of electromagnetic (EM) energy by a classical magnetic moment precessing about the magnetic field, or quantum mechanically, as absorption of photons with frequency equal to the Zeeman splitting. The absorption rate w of an incident EM wave (with frequency Ω and amplitudes of the electric and magnetic fields $\vec{E}^{\rm em}$ and $\vec{B}^{\rm em}$, correspondingly) is given by the Kubo formula [4–6]

$$w = 2\sum_{ij}\left[\sigma'_{ij}(\Omega)E_i^{\rm em}E_j^{\rm em} + \Omega\chi''_{ij}(\Omega)B_i^{\rm em}B_j^{\rm em}\right], \qquad (1)$$

where $\sigma'_{ij}(\Omega)$ is the real part of the conductivity and $\chi''_{ij}(\Omega)$ is the imaginary part of the spin susceptibility.

If the static magnetic field ($\vec{B}$) is in the plane of a two-dimensional electron gas (2DEG) and there is no spin-orbit coupling (SOC), the only resonant feature is due to a pole in the second term of Eq. (1) at the Larmor frequency. This is a conventional (or direct) ESR. However, because the spin susceptibility is proportional to $1/c^2$, where c is the speed of light, the direct ESR signal is very weak. SOC of Rashba [7,8] and/or Dresselhaus [9,10] types changes the situation drastically by producing an effective magnetic field, which acts on the spin of an electron with given momentum $\vec{p}$ and is proportional to $|\vec{p}|$. The driving electric field (either from a dc current or EM wave) gives rise to a flow of electrons with a nonzero drift momentum; hence the electron system as a whole experiences an effective magnetic field due to SOC. The magnitude of bare SOC is strongly enhanced by virtual interband transitions [11]; as a result, the electric component of an EM field couples to electron spins much stronger than the magnetic one. This is an electric dipole spin resonance (EDSR) [12–15], which gives rise to a range of spectacular phenomena, e.g., a strong enhancement of microwave absorption in a geometry when $\vec{E}^{\rm em}$ is in the plane of a 2DEG [16] and a shift of the resonance frequency by a dc current [3,5].

In this article, we discuss the effect of the electron-electron interaction on the ESR signal. In the Fermi-liquid (FL) language, ESR in the absence of SOC is an excitation of the Silin-Leggett (spin-flip) collective mode [17,18]; cf. Fig. 1(a). Although the very existence of this dispersive mode is due to many-body correlations, its end point at $q = 0$—the Larmor frequency—is protected from renormalizations by these correlations and given by the bare Zeeman energy [19]. In addition, there is a continuum of spin-flip single-particle excitations [shaded region in Fig. 1(a)], whose end point corresponds to the renormalized Zeeman energy. Although the absorption rate should, in principal, contain the contributions from both the collective mode and continuum, the latter does not contribute to ESR because its spectral weight vanishes at $q = 0$. These two main features of the ESR signal—no many-body renormalization of the resonance frequency and no contribution from the continuum—are due to conservation of the total spin ($\vec{S}$) projection onto $\vec{B}$.

The situation changes drastically in the presence of SOC, which breaks conservation of $\vec{S}\cdot\vec{B}$ and thus gives rise to fundamentally new features in the excitation spectrum discussed in this article. (Modification of the ESR spectrum due to both SOC and electron-electron interaction in the quantum Hall regime was considered in Ref. [20] within the Hartree-Fock theory.) Depending on whether the ratio of the Zeeman energy to spin-orbit splitting is larger than, comparable with, or smaller than unity, one can define the regimes of "high," "moderate," and "weak" magnetic fields. We show that the ESR frequency in the high-field regime is affected both by SOC and many-body correlations and scales nonlinearly with B [see Fig. 1(b)]. The deviation from linearity can be used to extract the amplitudes of both SOC and electron-electron correlations. In addition to the resonance peak, the ESR signal now also shows a broad feature due to the continuum of spin-flip excitations. In the presence of SOC, the resonance itself is entirely a many-body effect; in the absence of interactions, the signal comes entirely from the continuum [21]. The conventional ESR regime is reached in the limit of $B \to \infty$. As the field gets weaker, the ESR frequency scales down and finally vanishes at a critical field B_c, where the spin-split energy levels become degenerate [see insets in Fig. 1(b)] and the gap in the continuum closes. The region around B_c defines the moderate-field range. For $B < B_c$, the resonance appears again and two more modes split off the continuum as the field passes through the critical values, B_{c_2} and B_{c_1}. At $B \to 0$, the three modes evolve into chiral-spin resonances—collective oscillations of magnetization in the absence of the magnetic field [4,22,23]. In the most general

 ©2016 American Physical Society

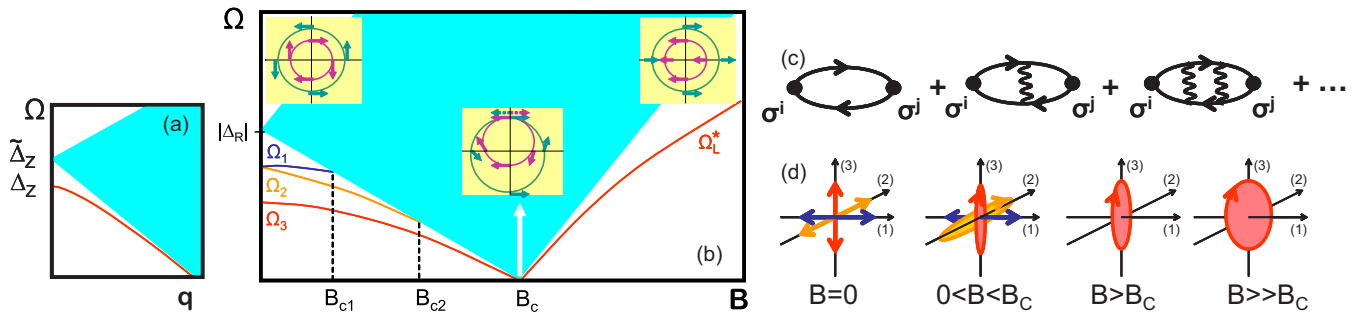

FIG. 1. (a) The Silin-Leggett mode (red) and continuum of spin-flip excitations (shaded, blue) for a Fermi liquid in the magnetic field. Δ_Z and $\tilde{\Delta}_Z$ are the bare and renormalized Zeeman energies, correspondingly. (b) Schematically: the frequencies of the collective modes and continuum boundaries as a function of B for a Fermi liquid with Rashba spin-orbit coupling in the magnetic field. The gap in the continuum closes at the critical field B_c, where the spin-split bands become degenerate. For $B < B_c$, there are three chiral-spin modes, $\Omega_{1...3}$. For $B > B_c$, there is one mode with a renormalized Larmor frequency, Ω_L^*. Insets: spin-split Fermi surfaces. (c) RPA diagrams for the spin susceptibility. (d) Evolution of polarizations of the collective modes with B.

case of both Rashba and Dresselhaus SOC present, all three chiral-spin modes are ESR-active.

In the prior literature, the discussion of the effect of SOC on ESR was largely limited to two aspects: D'yakonov-Perel' damping [24] of the signal [25,26] and coupling of electron spins to the electric field via the EDSR mechanism. We show in this article that the effect of SOC is much richer than the two aspects mentioned above. To the best of our knowledge, all the experiments thus far have been performed in the high-field limit, where the effect of SOC is quantitative rather than qualitative. We propose to study ESR in moderate and weak-field regimes, where the SOC-induced changes are qualitative.

II. MODEL AND FORMALISM

We study a two-dimensional (2D) electron system with both Rashba and Dresselhaus types of SOC (RSOC and DSOC, correspondingly) and in the presence of an in-plane magnetic field. We adopt the form of Dresselhaus SOC appropriate for a GaAs [001] quantum well and choose the x_1 and x_2 axes to be along the $[1\bar{1}0]$ and [110] directions, correspondingly. The single-particle part of the Hamiltonian then reads [27]

$$\hat{\mathcal{H}}_0 = \frac{\vec{k}^2}{2m}\hat{\sigma}_0 + \alpha(\hat{\sigma}_1 k_2 - \hat{\sigma}_2 k_1) + \beta(\hat{\sigma}_1 k_2 + \hat{\sigma}_2 k_1) - \frac{g\mu_B}{2}\hat{\sigma}_1 B, \quad (2)$$

where m is the band mass, μ_B is the Bohr magneton, $\hat{\sigma}_{1,2,3}$ are the Pauli matrices, $\hat{\sigma}_0$ is the 2×2 identity matrix, and α (β) is the Rashba (Dresselhaus) coupling constant. For simplicity, we chose the magnetic field to be along one of the two high-symmetry directions, i.e., $\vec{B} \,||\, \hat{x}_1$. This restriction will be relaxed in Sec. III C.

The many-body part of the Hamiltonian, $\hat{\mathcal{H}}_{\rm int}$, depends only on the electron positions, $\hat{\vec{x}}$. Consequently, $[\hat{\mathcal{H}}_{\rm int}, \hat{\vec{x}}] = 0$ and the velocity operator $\hat{\vec{v}} = i[\hat{\mathcal{H}}_0 + \hat{\mathcal{H}}_{\rm int}, \hat{\vec{x}}] = i[\hat{\mathcal{H}}_0, \hat{\vec{x}}]$ retains its free-electron form:

$$\hat{\vec{v}} = \left(\frac{k_1}{m}\hat{\sigma}_0 - (\alpha-\beta)\hat{\sigma}_2, \frac{k_2}{m}\hat{\sigma}_0 + (\alpha+\beta)\hat{\sigma}_1\right). \quad (3)$$

The gradient (k_1/m and k_2/m) terms in $\hat{\vec{v}}$ give rise to the Drude part of the conductivity, while the spin-dependent terms give rise to its B-dependent part, σ_B, which determines the EDSR signal. In the Voigt geometry ($\vec{E}^{\rm em} \,||\, \vec{B} \perp \vec{B}^{\rm em}$), the first (EDSR) term in the absorption rate [Eq. (1)] contains the component $(\sigma_B')_{11}$, which is related to the spin susceptibility via

$$(\sigma_B')_{11} = \frac{e^2}{(g\mu_B)^2\Omega}(\alpha-\beta)^2\chi_{22}'', \quad (4)$$

while the second (ESR) term contains $\chi''_{22/33}$ for $\vec{B}^{\rm em} \,||\, \hat{x}_{2/3}$. Equation (4) also holds in the presence of the electron-electron interaction. The ratio of the EDSR amplitude to the ESR one is given by $e^2(\alpha-\beta)^2/\mu_B^2\Omega_{\rm res}^2$, where $\Omega_{\rm res}$ is the resonance frequency. For the chiral-spin modes, $\Omega_{\rm res} \sim |\alpha-\beta|k_F$ and the ratio of the amplitudes is of the order of $(\lambda\!\!\!^{-}_F/\lambda\!\!\!^{-}_C)^2 \sim 10^8$–$10^9$, where $\lambda\!\!\!^{-}_F$ is the Fermi wavelength and $\lambda\!\!\!^{-}_C = \hbar/m_e c$ is the Compton length (m_e is the free electron mass) [4]. For the Silin-Leggett mode, $\Omega_{\rm res} = g\mu_B B \equiv \Omega_L$ and the EDSR/ESR ratio is $(\lambda\!\!\!^{-}_F/\lambda\!\!\!^{-}_C)^2 \times (\Delta_{\rm SOC}/\Omega_L)^2$, where $\Delta_{\rm SOC}$ is the characteristic spin-orbit splitting and Ω_L is the Larmor frequency.

In this work, we assume that the EDSR part of the signal dominates the ESR one, so that the absorption rate in Eq. (1) is determined by $(\sigma_B')_{11}$ to very high accuracy. We also assume that both the spin-orbit splitting and Zeeman energy are much smaller than the Fermi energy. In this case, the corresponding terms in the Hamiltonian can be treated as corrections to the conventional, SU(2)-invariant FL, and the complications encountered in generalizing the FL theory for arbitrarily large spin-dependent terms [28,29] do not arise. The ESR signal is completely characterized by the spin susceptibility. At $q = 0$, the spin and charge sectors of the theory decouple because of charge conservation [23], and $\chi_{ij}(\Omega)$ can be found within the usual random-phase approximation (RPA), in which the Green's functions include the B-dependent shifts of the chemical potential [see Fig. 1(c)]. For an s-wave interaction ($U = \text{const}$), the Matsubara form of χ_{ij} is given by the matrix product [23]

$$\chi_{ij}(\Omega_m) = -\frac{(g\mu_B)^2}{4}\Pi^0_{ij'}(\Omega_m)\left[1 + \frac{U}{2}\hat{\Pi}^0(\Omega_m)\right]^{-1}_{j'j}, \quad (5)$$

where $\Pi^0_{ij}(\Omega_m) = \int_K \mathrm{Tr}[\hat{\sigma}_i \hat{G}_K \hat{\sigma}_j \hat{G}_{K+Q}]$ with $i,j \in \{1,2,3\}$, $Q = (i\Omega_m, \vec{0})$; $K = (i\omega_m, \vec{k})$; and $\int_K \equiv T\sum_{\omega_m} \int \frac{d^2k}{(2\pi)^2}$. Furthermore, $\hat{G}_K^{-1} = (i\omega + \mu)\hat{\sigma}_0 - \hat{\mathcal{H}}'_0$, where $\hat{\mathcal{H}}'_0$ differs from $\hat{\mathcal{H}}_0$ in that the Zeeman energy is replaced by its renormalized value (see Appendix A): $g\mu_B B \to g\mu_B B/(1-u)$, where $u \equiv \nu_{2D} U$ is the dimensionless coupling constant and $\nu_{2D} = m/2\pi$ is the density of states in 2D. For weak SOC, i.e., for $|\alpha|$, $|\beta| \ll v_F$ with v_F being the Fermi velocity in the absence of SOC, the system is characterized by four energy scales:

$$\Delta_R \equiv 2\alpha k_F; \Delta_D \equiv 2\beta k_F; \Delta_Z \equiv g\mu_B B; \tilde{\Delta}_Z = \frac{\Delta_Z}{1-u}, \quad (6)$$

where $k_F = m v_F$. We choose the Zeeman energies to be positive, while the signs of Δ_R and Δ_D are arbitrary.

We note in passing that RPA for the case of an s-wave interaction gives the same results as the kinetic equation for a FL with a Landau function that contains only the zeroth angular harmonic in the spin channel (see Appendix D).

III. THE ESR SPECTRUM: MANY-BODY DESCRIPTION

A. ESR without spin-orbit coupling

We start by revisiting the well-known case of a FL without SOC in the magnetic field [$\alpha = \beta = 0$ in Eq. (2)]. In this case, $\Pi^0_{1j}(\Omega_m) = 0$ ($j \in \{1,2,3\}$) because the projection of spin on the direction of $\vec{B}$ is conserved. For the rest of the components we obtain, upon analytic continuation ($i\Omega_m \to \Omega + i0^+$), $\Pi^0_{22}(\Omega) = \Pi^0_{33}(\Omega) = 2\nu_{2D}\tilde{\Delta}_Z^2/(\Omega^2 - \tilde{\Delta}_Z^2)$ and $\Pi^0_{23}(\Omega) = -\Pi^0_{32}(\Omega) = -2i\nu_{2D}\Omega\tilde{\Delta}_Z/(\Omega^2 - \tilde{\Delta}_Z^2)$. The collective mode corresponds to a pole of Eq. (5), when $\det[1 + \frac{U}{2}\Pi^0_{ij}(\Omega)] = 0$ or $1 + \frac{U}{2}\Pi^0_{22} = \pm\frac{U}{2} i\Pi^0_{23}$. The only solution of this equation outside the spin-flip continuum is the Larmor frequency: $\Omega_L = \tilde{\Delta}_Z(1-u) = \Delta_Z$. On the other hand, $\chi''_{ij}(\Omega)$ vanishes at the continuum ($\Omega = \tilde{\Delta}_Z$), and thus the continuum does not contribute to ESR.

B. ESR with Rashba spin-orbit coupling

This case is realized by setting $\beta = 0$ in Eq. (2). After including the self-energy correction to the Zeeman term [30] (see Appendix A), the dispersions of the spin-split bands become $\varepsilon^{\pm}_{\vec{k}} = k^2/2m \pm \frac{1}{2}\sqrt{(2\alpha k)^2 + (\tilde{\Delta}_Z)^2 - 2\tilde{\Delta}_Z(2\alpha k)\sin\theta_k}$, where θ_k is the angle between $\vec{k}$ and the x_1 axis. Although the spin projection onto $\vec{B}$ is not conserved anymore, some off-diagonal components of Π^0_{ij} still vanish. Indeed, since $\vec{B}^{\mathrm{em}} \times \vec{B} = 0$ for $\vec{B}^{\mathrm{em}} \parallel \vec{B} \parallel \hat{x}_1$, the only two pseudovectors in the system are $\vec{B}^{\mathrm{em}}$ and $\vec{B}$ themselves. The magnetization induced by $\vec{B}^{\mathrm{em}}$ is also a pseudovector and thus can only be parallel to $\vec{B}$, which implies that $\Pi^0_{1j} = 0$ for $j = 2,3$. The nonzero components of $\hat{\Pi}^0$ are given by (see Appendix B)

$$\Pi^0_{11}(\Omega) = -2\nu_{2D}\frac{W^2(1-f)}{4\tilde{\Delta}_Z^2},$$

$$\Pi^0_{22}(\Omega) = -2\nu_{2D}\left[\frac{\tilde{\Delta}_Z^2}{fW^2} + \left(1 - \frac{1}{f}\right)\left(1 - \frac{W^2}{4\tilde{\Delta}_Z^2}\right)\right],$$

$$\Pi^0_{33}(\Omega) = -2\nu_{2D}\left[1 + \frac{\Omega^2}{fW^2}\right],$$

$$\Pi^0_{23}(\Omega) = 2\nu_{2D}\frac{i\Omega}{\tilde{\Delta}_Z}\left[\frac{1}{2}\left(1 - \frac{1}{f}\right) + \frac{\tilde{\Delta}_Z^2}{fW^2}\right] = -\Pi^0_{32}(\Omega), \quad (7)$$

where $f \equiv \sqrt{1 - 4\Delta_R^2\tilde{\Delta}_Z^2/W^4}$ and $W^2 \equiv \Delta_R^2 + \tilde{\Delta}_Z^2 - \Omega^2 - i0^+\mathrm{sgn}\Omega$. The formulas above reduce to the known limits [23] when $\Delta_R \to 0$ and $\Delta_Z \to 0$, respectively.

The subband energies vary around the Fermi surface, reaching the maximum and minimum values of $|\tilde{\Delta}_Z \pm |\Delta_R||$, correspondingly. As a result, the continuum of spin-flip excitations occupies a finite interval of frequencies $|\tilde{\Delta}_Z - |\Delta_R|| < \Omega < \tilde{\Delta}_Z + |\Delta_R|$, where all Π^0's in Eq. (7) have nonzero imaginary parts. This is in contrast to the case of $\alpha = 0$, where the continuum has zero spectral weight [see Fig. 1(a)]. The gap in the continuum closes at a special field B_c such that $\tilde{\Delta}_Z(B_c) = |\Delta_R|$ and the spin-split bands become degenerate [Fig. 1(b)].

The collective modes correspond to the poles of Eq. (5) outside the continuum. The eigenmode equation splits into two:

$$1 + \frac{U}{2}\Pi^0_{11}(\Omega) = 0, \quad (8a)$$

$$\left[1 + \frac{U}{2}\Pi^0_{22}(\Omega)\right]\left[1 + \frac{U}{2}\Pi^0_{33}(\Omega)\right] = -\frac{U^2}{4}\left[\Pi^0_{23}(\Omega)\right]^2. \quad (8b)$$

For $B > B_c$, Eq. (8a) has no solutions while Eq. (8b) has a unique solution (see Appendix C), which is the Larmor frequency, Ω^*_L, renormalized both by SOC and electron-electron interaction [cf. inset in Fig. 2(a)]. At the highest fields ($\tilde{\Delta}_Z \gg |\Delta_R|/u$),

$$\Omega^*_L \approx \Delta_Z\left[1 - \frac{(2-3u)(1-u)}{4u}\left(\frac{\Delta_R}{\Delta_Z}\right)^2\right]. \quad (9)$$

When B is just slightly above B_c, i.e., $\tilde{\Delta}_Z \approx |\Delta_R|$ but still $\tilde{\Delta}_Z > |\Delta_R|$, we get

$$\Omega^*_L \approx (\tilde{\Delta}_Z - |\Delta_R|)\left[1 - \frac{u^2\left(1 - \frac{3u}{4}\right)^2}{2\left(1 - \frac{u}{2}\right)^2(1-u)^2}\frac{(\tilde{\Delta}_Z - |\Delta_R|)^2}{\tilde{\Delta}_Z^2}\right]. \quad (10)$$

In the limit of $u \ll 1$, we have an additional regime defined by $\Delta_R \ll \tilde{\Delta}_Z \ll \Delta_R/u$, where

$$\Omega^*_L \approx |\tilde{\Delta}_Z|\left[1 - \frac{u^2\tilde{\Delta}_Z}{2|\Delta_R|}\right]. \quad (11)$$

For $B < B_c$, Eq. (8a) has one solution, $\Omega = \Omega_1$, which corresponds to oscillations of the x_1 component of the magnetization $\vec{M}$, while Eq. (8b) has two solutions, $\Omega = \Omega_2$ and $\Omega = \Omega_3$, which correspond to coupled oscillations of the components M_2 and M_3. The Ω_1 and Ω_2 modes run into the continuum at fields B_{c_1} and B_{c_2}, correspondingly [cf. Fig. 1(b)]. The three modes are plotted in Fig. 2(a) for a range of fields below B_c. As the field is lowered further, these three solutions evolve into the spin-chiral resonances [4,22]. At $B = 0$, Π^0_{23} in Eq. (8b) vanishes by time-reversal symmetry, while Π^0_{11}

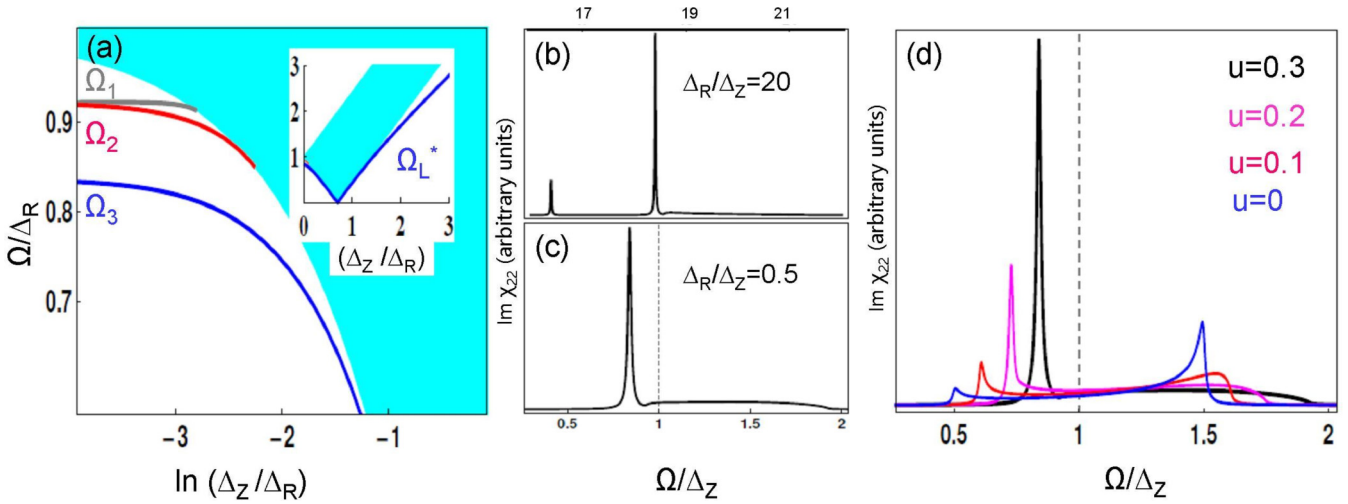

FIG. 2. (a) Chiral-spin modes as a function of the Zeeman energy, Δ_Z, in units of the Rashba spin splitting, Δ_R (on a semilogarithmic scale). Inset: renormalized Larmor mode (Ω_L^*) at higher fields. (b) Imaginary part of the susceptibility in the weak-field limit ($\Delta_R/\Delta_Z = 20$). (c) Same as in the high-field limit. The dashed line marks the bare Larmor frequency (Ω_L). The continuum is seen as a broad hump to the right of the resonance. In panels (a)–(c), the dimensionless interaction is $u = 0.3$. (d) Evolution of the ESR signal with u. Here $\Delta_R/\Delta_Z = 0.5$. Damping of $\Gamma = 0.01\Delta_R$ was added to the Green's functions to mimic the effect of disorder in all plots.

and Π^0_{22} become equal by the $C_{\infty v}$ symmetry. In this limit, $\Omega_1 = \Omega_2 = |\Delta_R|\sqrt{1-u/2}$ and $\Omega_3 = |\Delta_R|\sqrt{1-u}$ [23].

In the absence of DSOC, absorption is determined entirely by χ''_{22} [cf. Eq. (4)]. Since the Ω_1 mode is decoupled from the Ω_2 and Ω_3 modes, it is ESR-silent. The magnetic field couples the Ω_2 and Ω_3 modes, both of which show up in ESR. For $B > B_c$, there is only one ESR-active mode, whereas for $B < B_c$ there can be one or two active modes, depending of whether B is smaller or larger than B_{c_2}. In addition to a sharp peak(s), there is also a broad feature corresponding to absorption by the continuum of spin-flip excitations.

Figure 2(d) depicts the evolution of the ESR signal with increasing u. In the presence of SOC, a sharp mode occurs only due to many-body interaction, as it pushes the mode away from the continuum. This is in contrast to the case without SOC, where the mode exists even without interaction. Both the peak and broad hump due to the continuum have been observed in Ref. [38], although the detailed shape of the hump is yet to be explained.

As the magnetic field increases from zero to values exceeding B_c, polarization of the collective modes changes qualitatively [cf. Fig. 1(d)]. At $B = 0$, the susceptibility is

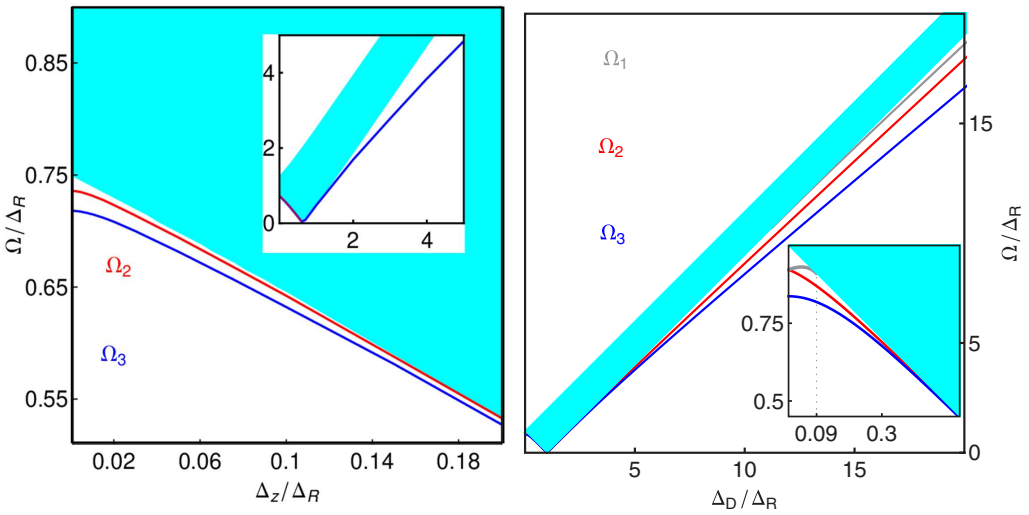

FIG. 3. Left: Collective modes in the presence of the magnetic field, and both Rashba and Dresselhaus spin-orbit coupling. $\beta/\alpha = -0.25$. Below the field at which the gap in the continuum closes, there are two chiral-spin modes; above this field there is only one precessing mode. All the modes in this case are elliptically polarized. Inset: zoom of the high-field region. Right: Collective modes in the presence of Rashba and Dresselhaus spin-orbit coupling but in the absence of the magnetic field. There are three modes on either side of the gap closing point. The entire structure of the collective mode is symmetric under $\alpha \to \beta$. All three modes are linearly polarized. Inset: zoom of the region $|\Delta_D| \ll |\Delta_R|$. $u = 0.3$ in both plots.

TABLE I. SOC parameters for some common quantum wells. Mn doping in $Cd_{1-x}Mn_xTe$ provides an additional field to the 2DEG due to the localized moments on Mn. The range in g for this material is controlled by Mn doping.

Material	n (10^{11} cm^{-2})	$\|g$ factor$\|$	α (meV Å)	$\Delta_R = \frac{2\alpha k_F}{g\mu_B}$ (T)	β (meV Å)	$\Delta_D = \frac{2\beta k_F}{g\mu_B}$ (T)	References
SiGe/Si/SiGe	1–7	2	0.055	$7.5–19.9 \times 10^{-3}$			[36]
$Mg_xZn_{1-x}O$/ZnO	2.1	1.94	0.7	0.15			[37]
$Cd_{1-x}Mn_xTe$	3.5	1.6–5	3.3	0.34–1.1	4.6	0.47–1.5	[38]
GaAs/AlGaAs	2.3	0.445	3.1	2.89	0.55	0.51	[39]
GaAs/AlGaAs	5.8	0.27	1.5	3.7	1.4	3.4	[40]
GaAs/AlGaAs	1.4–7	0.4	5	4.0–9.1	4	3.2–7.2	[41]
InAs	21	7.8–8.7	67	9.7–10.8	3.5	0.5–0.6	[42,43]
InAs	11–20	8	60	6.8–9.2			[44]
$In_{1-x}Ga_xAs/In_{1-y}Al_yAs$	17–24	4	65–92	21.6–25.9			[45]

diagonal, which means that the different components of the magnetization oscillate independently and are thus linearly polarized. For $0 < B < B_c$, the M_1 component is still linearly polarized, while coupled oscillations of the M_2 and M_3 components can be decomposed into two elliptically polarized modes. For $B > B_c$, there is only one elliptically polarized mode which evolves into a circularly polarized Silin-Leggett mode for $B \gg B_c$.

C. ESR with both Rashba and Dresselhaus spin-orbit coupling

Adding DSOC to RSOC lowers the symmetry from $C_{\infty v}$ to C_{2v}. As a result, the doubly degenerate spin-chiral resonance splits into two already at $B = 0$. Other than that, DSOC does not change the situation qualitatively, as long as $\vec{B}$ is along the high-symmetry axis [as in Eq. (2)]: one of the three modes is still ESR-silent, so the signal consists of up to two lines. If $\vec{B}$ is along a generic in-plane direction [which means that $\hat{\sigma}_1 B_1$ in Eq. (2) changes to $\hat{\sigma}_1 B_1 + \hat{\sigma}_2 B_2$], all modes become ESR-active, and the signal consists of up to three lines. This case can only be tackled by a numerical treatment of the general equations presented in Appendix B. Figure 3 (left) shows collective modes of a system with both RSOC and DSOC and with the field oriented at 45° to the x_1 axis, such that $B_1 = B_2 = B$. The RSOC and DSOC couplings are chosen in such a way that there are only two collective modes at $B = 0$.

D. ESR with Rashba and Dresselhaus spin-orbit couplings in zero field

For completeness, we also discuss the chiral-spin resonances in the zero-field limit but in the presence of both Rashba and Dresselhaus couplings. (The case when only one type of SOC is present has been thoroughly analyzed in the prior literature; see Refs. [4,22,23].) In the absence of field, the time-reversal symmetry is intact and thus collective modes can only be linearly polarized. Figure 3 (right) shows the collective modes as a function of the Dresselhaus coupling β (parametrized as $\Delta_D \equiv 2\beta k_F$). Although the evolution of the spectrum with the ratio Δ_D/Δ_R is qualitatively similar to the evolution with Δ_Z/Δ_R in the $B \neq 0$ case (in terms of closing and reopening the gap in the continuum), there are crucial differences between these two cases, namely, (1) the $B = 0$ spectrum is symmetric about the zero-gap point, whereas it is asymmetric in the $B \neq 0$ case; (2) the modes are linearly polarized in the $B = 0$, whereas they are elliptically polarized in the $B \neq 0$. These results for the $B = 0$ case can be derived analytically; see Appendix B 2.

IV. CONCLUSIONS

We presented a many-body theory of the ESR/EDSR effects in the presence of SOC of both Rashba and Dresselhaus types. The combined effect of the electron-electron and spin-orbit interactions leads to a splitting of the resonance into up to three lines, which should be observable in an experiment. These multiple resonances are the optical (massive) collective modes of a Fermi liquid subject to both external and spin-orbit magnetic fields. We have also shown that the Silin-Leggett mode is affected by the electron-electron interaction in the presence of SOC; this effect must be accounted for when extracting the g factors and SOC parameters from the precession measurements [33–35].

The best platform for observing the effects predicted in this paper are the semiconductor heterostructures in the regime when the SOC energy splitting is comparable to the Zeeman splitting due to an in-plane magnetic field. In Table I, we provide a summary of relevant material parameters for some of the conventional heterostructures. The Rashba and Dresselhaus SOC energy scales are presented in units of Teslas to give an idea of the strength of the field required to probe the multiple-resonance regime of the spectrum. Recent advances in microwave technology [46] have greatly broadened the range of frequencies thus making ESR a promising tool for the detection of the chiral-spin modes.

ACKNOWLEDGMENTS

We would like to thank C. R. Bowers, I. Paul, F. Perez, E. I. Rashba, and C. A. Ullrich for useful discussions. S.M. acknowledges a Dirac Fellowship award from the NHMFL, which is supported by the NSF via Cooperative Agreement No. DMR-1157490, the State of Florida, and the US DOE. D.L.M. acknowledges support from the NSF via Grant No. NSF DMR-1308972 and a Stanislaw Ulam Scholarship at the Center for Nonlinear Studies, Los Alamos National Laboratory. We acknowledge the hospitality of the Kavli Institute for Theoretical Physics, which is supported by the NSF via Grant No. NSF PHY11-25915.

APPENDIX A: SINGLE-PARTICLE HAMILTONIAN: EIGENSTATES AND SELF-ENERGY CORRECTION

In this Appendix, we derive the form of the self-energy that enters the Green's functions in the calculation of the polarization tensor. It is convenient to start with the Hamiltonian in Eq. (2) which can be rewritten as

$$\hat{\mathcal{H}}_0 = \frac{\vec{k}^2}{2m}\hat{\sigma}_0 + \lambda_{\vec{k}} k(\sin\phi_k \hat{\sigma}_1 - \cos\phi_k \hat{\sigma}_2). \tag{A1}$$

The parameters $\lambda_{\vec{k}}$ and ϕ_k are defined by the following relations:

$$\begin{aligned} 2\lambda_{\vec{k}} k &= \sqrt{(2\alpha k)^2 + (2\beta k)^2 - 8\alpha\beta k^2 \cos 2\theta_k + (g\mu_B B)^2 - 4(g\mu_B B)(\alpha+\beta)k\sin\theta_k}, \\ \sin\phi_k &= \frac{\alpha+\beta}{\lambda_{\vec{k}}}\sin\theta_k - \frac{g\mu_B B}{2\lambda_{\vec{k}} k}, \\ \cos\phi_k &= \frac{\alpha-\beta}{\lambda_{\vec{k}}}\cos\theta_k, \end{aligned} \tag{A2}$$

where θ_k is the azimuthal angle $\vec{k}$ with respect to the x_1 axis. The eigenvalues and eigenvectors are given by

$$\varepsilon^{\pm}_{\vec{k}} = \frac{k^2}{2m} \pm \lambda_{\vec{k}}, \tag{A3}$$

$$|\vec{k},\pm\rangle = \frac{1}{\sqrt{2}}\begin{pmatrix} 1 \\ \mp i e^{i\phi_k} \end{pmatrix}. \tag{A4}$$

To account for renormalization of the Zeeman energy and spin-orbit parameters entering the Green's function, one needs to find the momentum- and frequency-independent part of the self-energy, $\hat{\Sigma}$. For an s-wave interaction ($U = \text{const}$), $\hat{\Sigma}$ can be found in the self-consistent Born approximation as

$$\hat{\Sigma} = -U\int_K \hat{G}_K, \quad \hat{G}_K = \left(\left[\hat{G}^0_K\right]^{-1} - \hat{\Sigma}\right)^{-1}, \tag{A5}$$

where $[\hat{G}^0_K]^{-1} = (i\omega_m + \mu)\hat{\sigma}_0 - \hat{\mathcal{H}}_0$. By construction, $\hat{\Sigma}$ does not depend on K and thus can be written as

$$\hat{\Sigma} = \sum_{i=1\ldots3} a_i \hat{\sigma}_i, \tag{A6}$$

where the coefficients a_i are to be determined. Note that we dropped the coefficient a_0 as it would only result in a shift of the chemical potential. Solving the algebraic matrix equation, we get $a_1 = \frac{u}{1-u}\frac{g\mu_B B}{2}$ (where $u \equiv \frac{mU}{2\pi}$), and $a_2 = a_3 = 0$. This amounts to changing $g\mu_B B \to \frac{g\mu_B B}{1-u}$ or $\Delta_Z \to \tilde{\Delta}_Z$. Since $a_2 = a_3 = 0$, the spin-orbit parameters are not renormalized. This is a special feature of the s-wave interaction approximation.

The Green's function (with the self-energy correction) is then explicitly written as

$$\hat{G}_K = \sum_{r\pm} g^r_K \hat{\Omega}_r, \quad \hat{\Omega}_r = \frac{1}{2}[\hat{\sigma}_0 + r(\hat{\sigma}_1 \sin\phi_k - \hat{\sigma}_2\cos\phi_k)], \tag{A7}$$

where $g^r_K = 1/(i\omega_m - \tilde{\varepsilon}^r_{\vec{k}})$ and $\tilde{\varepsilon}^r_{\vec{k}}$ is the electron dispersion which contains the renormalized Zeeman energy: $\Delta_Z \to \tilde{\Delta}_Z$.

APPENDIX B: COLLECTIVE MODES WITHIN THE RANDOM-PHASE APPROXIMATION

1. General case

In this Appendix, we provide some details of the calculation of the spin-charge polarization tensor Π^0_{ij}, which is needed to find the collective modes within the random-phase approximation (RPA). This is a challenging task in the most general case, when the magnetic field and both Rashba and Dresselhaus types of spin-orbit coupling (RSOC and DSOC, correspondingly) are present. However, in the limit when both the magnetic field and SOC are weak, i.e., when the Zeeman energy and spin-orbit splitting of the energy bands are small compared to the Fermi energy, one can confine the momentum integration to the vicinity of the Fermi surface and carry out some of the steps analytically.

We choose the magnetic field to be along an arbitrary in-plane direction. Consequently, the Zeeman term in Eq. (2) is replaced by $-(g\mu_B/2)(\hat{\sigma}_1 B_1 + \hat{\sigma}_2 B_2)$. The corresponding changes in the eigenvalues and eigenvectors can readily be traced down; we will refrain from giving explicit forms here. Linearizing the dispersion near the Fermi energy as $\varepsilon^{\pm}_{\vec{k}} - \mu = \xi \pm \Lambda_{\theta_k}$, where $\Lambda_{\theta_k} \equiv 2\lambda_{k=k_F,\theta_k} k_F$ is the SOC splitting at the point θ_k on the Fermi surface, we arrive at two types of integrals [here, k_F is the Fermi momentum in the absence of both the magnetic field and SOC and Q stands for the $2+1$ bosonic momentum with the zero spatial part: $Q = (i\Omega_m, 0)$]:

$$\begin{aligned} &\frac{1}{2}\int d\xi (g^+_K g^-_{K+Q} + g^-_K g^+_{K+Q}) \\ &\quad = \frac{1}{2}\int d\xi \left\{ \frac{n_F(\varepsilon^+_{\vec{k}}) - n_F(\varepsilon^-_{\vec{k}})}{i\Omega_m + \varepsilon^+_{\vec{k}} - \varepsilon^-_{\vec{k}}} + (+\to -)\right\} \\ &\quad = -\frac{\Lambda^2_{\theta_k}}{\Omega^2_m + \Lambda^2_{\theta_k}} \end{aligned} \tag{B1}$$

and

$$\frac{1}{2}\int d\xi (g^+_K g^-_{K+Q} - g^-_K g^+_{K+Q}) = \frac{i\Omega_m \Lambda_{\theta_k}}{\Omega^2_m + \Lambda^2_{\theta_k}}. \tag{B2}$$

A general form of $\lambda_{\vec{k}}$ is obtained from Eq. (A1) by adding the second component of the magnetic field, which amounts to replacing $\sin\phi_k$ by $\frac{\alpha+\beta}{\lambda_{\vec{k}}}\sin\theta_k - \frac{g\mu_B B_1}{2\lambda_{\vec{k}} k}$ and $\cos\phi_k$ by

$(\alpha-\beta)\cos\theta_k/\lambda_{\vec{k}} + g\mu_B B_2/(2\lambda_{\vec{k}}k)$ in Eq. (A2). Using these relations, we get

$$\begin{aligned}
\Pi^0_{11}(\Omega_m) &= -2\nu_{2D}\int \frac{d\theta_k}{2\pi}\frac{\Lambda^2_{\theta_k}}{\Omega_m^2+\Lambda^2_{\theta_k}}\cos^2\phi_k,\\
\Pi^0_{12}(\Omega_m) &= -\nu_{2D}\int \frac{d\theta_k}{2\pi}\frac{\Lambda^2_{\theta_k}}{\Omega_m^2+\Lambda^2_{\theta_k}}\sin 2\phi_k,\\
\Pi^0_{21}(\Omega_m) &= \Pi^0_{12}(\Omega_m),\\
\Pi^0_{13}(\Omega_m) &= 2\nu_{2D}\int \frac{d\theta_k}{2\pi}\frac{\Omega_m\Lambda_{\theta_k}}{\Omega_m^2+\Lambda^2_{\theta_k}}\cos\phi_k,\\
\Pi^0_{31}(\Omega_m) &= -\Pi^0_{13}(\Omega_m),\\
\Pi^0_{22}(\Omega_m) &= -2\nu_{2D}\int \frac{d\theta_k}{2\pi}\frac{\Lambda^2_{\theta_k}}{\Omega_m^2+\Lambda^2_{\theta_k}}\sin^2\phi_k,\\
\Pi^0_{23}(\Omega_m) &= 2\nu_{2D}\int \frac{d\theta_k}{2\pi}\frac{\Omega_m\Lambda_{\theta_k}}{\Omega_m^2+\Lambda^2_{\theta_k}}\sin\phi_k,\\
\Pi^0_{32}(\Omega_m) &= -\Pi^0_{23}(\Omega),\\
\Pi^0_{33}(\Omega_m) &= -2\nu_{2D}\int \frac{d\theta_k}{2\pi}\frac{\Lambda^2_{\theta_k}}{\Omega_m^2+\Lambda^2_{\theta_k}}.
\end{aligned} \tag{B3}$$

For Fig. 3, we considered the magnetic field to be at 45° to the x_1 axis, i.e., $B_1 = B_2 \equiv B$. Solutions of the eigenmode equation $\det[1+(U/2)\hat{\Pi}^0]=0$ are shown in the left panel of Fig. 3. In general, there are no qualitative differences compared to the case of only RSOC and the magnetic field: for $B<B_c$ there are two or three modes depending on the ratio α/β, whereas for $B>B_c$ there is only one mode. For $\alpha/\beta=-0.25$, as chosen in the left panel of Fig. 3, there are only two modes.

2. Collective modes in zero field

Here, we present details of the derivation of collective modes in the absence of B but in the presence of both RSOC and DSOC. In this case, the spin-flip continuum occupies the energy interval $|\Delta_R-\Delta_D|<\Omega<\Delta_R+\Delta_D$, where $\Delta_D \equiv 2\beta k_F$ (for definiteness we choose $\Delta_{R,D}>0$). The collective modes are well defined as they occur below the lower boundary of the continuum. The susceptibility is still a diagonal matrix so that its 11, 22, and 33 sectors are all decoupled. The nonzero elements of $\hat{\Pi}^0$ are (in real frequencies)

$$\begin{aligned}
\Pi^0_{11}(\Omega) &= F_1(\Omega)+F_2(\Omega),\\
\Pi^0_{22}(\Omega) &= F_1(\Omega)-F_2(\Omega),\\
\Pi^0_{33}(\Omega) &= 2F_1(\Omega),\\
\text{where}\quad F_1(\Omega) &= -\nu_{2D}\left[1+\frac{\Omega^2}{W_D^2}\right],\\
F_2(\Omega) &= -\nu_{2D}\frac{\Delta_R^2+\Delta_D^2}{2\Delta_R\Delta_D}\left[1+\frac{1}{W_D^2}\left(-\Omega^2-\frac{\left(\Delta_R^2-\Delta_D^2\right)^2}{\Delta_R^2+\Delta_D^2}\right)\right],
\end{aligned} \tag{B4}$$

and $W_D^2=\sqrt{[\Omega^2-(\Delta_R+\Delta_D)^2][\Omega^2-(\Delta_R-\Delta_D)^2]}$. The diagonal form of $\hat{\Pi}^0$ suggests that all the modes are linearly polarized. The eigenmode equation, $\det(1+U\hat{\Pi}^0/2)=0$, leads to the following three equations:

$$1+UF_1(\Omega)=0, \tag{B5}$$

$$1\pm\frac{u(\Delta_R\mp\Delta_D)^2}{4\Delta_R\Delta_D}\left(1-\sqrt{\frac{(\Delta_R\pm\Delta_D)^2-\Omega^2}{(\Delta_R\mp\Delta_D)^2-\Omega^2}}\right)=0. \tag{B6}$$

Solving those, we get the frequencies of the collective modes:

$$\begin{aligned}
&\Omega_i^2=(\Delta_R-\Delta_D)^2\left[1-\frac{uf_i}{2z_i}\right], i\in(1,2);\ \text{where}\\
&z_1=1+\frac{2\Delta_R\Delta_D}{u(\Delta_R-\Delta_D)^2}, z_2=1-\frac{2\Delta_R\Delta_D}{u(\Delta_R+\Delta_D)^2},\ f_1=1, f_2=\frac{(\Delta_R+\Delta_D)^2}{(\Delta_R-\Delta_D)^2}\left(1-\frac{4\Delta_R\Delta_D}{u(\Delta_R+\Delta_D)^2}\right)^2,\\
&\Omega_3^2=(\Delta_R-\Delta_D)^2\left[1-\frac{u^2}{1-2u}\frac{\sqrt{1+z_3+z_3\frac{\Delta_R^2+\Delta_D^2}{2\Delta_R\Delta_D}}-(1+z_3)}{z_3}\right],\ z_3=\left(\frac{u}{1-u}\right)^2\frac{(\Delta_R-\Delta_D)^2}{2\Delta_R\Delta_D}.
\end{aligned} \tag{B7}$$

These solutions are plotted in Fig. 3 (right) as a function of increasing DSOC. It follows from Eq. (B7) that Ω_1 and Ω_3 graze the continuum up to the gap-closing point, where $\Delta_R=\Delta_D$, whereas Ω_2 hits the continuum at a point where $f_2=0$, which is below the gap-closing point. The solution is symmetric under $\Delta_R \leftrightarrow \Delta_D$ and, as a result, there are three collective modes on each side of the gap-closing point.

APPENDIX C: EIGENMODE EQUATIONS FOR THE CASE WHEN BOTH RASHBA SPIN-ORBIT COUPLING AND MAGNETIC FIELD ARE PRESENT

In this Appendix, we analyze some properties of the eignemode equations for the case when RSOC and magnetic field are present.

1. Proving the absence of the collective mode in the 11 sector for $B > B_c$

The frequency of the collective mode in the 11 sector (corresponding to oscillations of magnetization along the x_1 axis, i.e., along the static magnetic field) is determined from Eq. (8a): $1 + \frac{U}{2}\Pi^0_{11}(\Omega) = 0$. Here, we prove that this equation has no solutions for $B > B_c$. Explicitly, this equation reads

$$\frac{1}{u} = \frac{(1-f)W^2}{4\tilde{\Delta}_Z^2}, \tag{C1}$$

where

$$f \equiv \sqrt{1 - 4\Delta_R^2\tilde{\Delta}_Z^2/W^4} \tag{C2}$$

and

$$W^2 \equiv \Delta_R^2 + \tilde{\Delta}_Z^2 - \Omega^2 - i0^+\mathrm{sgn}\Omega. \tag{C3}$$

Using the standard inequality of arithmetic and geometric means, we find that f is always real and <1, if we restrict ourselves to the region below the continuum boundaries, i.e., for $\Omega < |\tilde{\Delta}_Z - \Delta_R|$. This implies that the right-hand side (RHS) of Eq. (C1) is smaller than $\frac{W^2}{4\tilde{\Delta}_Z^2}$, which on its turn can be immediately seen to be less than $\frac{1}{2}$ for $\frac{\Delta_R}{\tilde{\Delta}_Z} < 1$, i.e, for $B > B_c$. Therefore, we have $0 < \mathrm{RHS} < 1/2$, while the left-hand side is larger than 1 within the paramagnetic phase ($u < 1$). Thus there is no solution of Eq. (C1) for $B > B_c$.

2. Collective modes in the 22 and 33 sectors

We now analyze Eq. (8b), which gives the collective modes in the 22 and 33 sectors, in the various limits and derive the results presented in Eqs. (9)–(11). Equation (8b) can be rewritten as

$$\frac{1}{u} = X + \frac{1}{1-u}Y, \tag{C4}$$

where

$$X \equiv \frac{\tilde{\Delta}_Z^2}{fW^2} - \frac{1}{4}\left(\frac{1}{f} - 1\right)\left(3 - \frac{\Delta_R^2}{\tilde{\Delta}_Z^2}\right), \tag{C5}$$

$$Y \equiv \frac{\Omega^2}{\tilde{\Delta}_Z^2}\left[\frac{\tilde{\Delta}_Z^2}{fW^2} - \frac{1}{4}\left(\frac{1}{f} - 1\right)\right]. \tag{C6}$$

To proceed further, we introduce the dimensionless quantities $w \equiv \Omega/\tilde{\Delta}_Z$ and $r \equiv |\Delta_R|/\tilde{\Delta}_Z$. We look for a solution of the form $w^2 = (1-r)^2 - \delta$, where δ is a new variable confined to $0 < \delta < (1-r)^2$. In these notations, $W^2/\tilde{\Delta}_Z^2 = 2r + \delta$ and $fW^2 = \sqrt{\delta}\sqrt{4r+\delta}$. The quantities X and Y can be rewritten as

$$\begin{aligned} X &= \frac{1}{ab} - \frac{3-r^2}{8}\frac{(a-b)^2}{ab}, \\ Y &= \left[\frac{1}{ab} - \frac{1}{8}\frac{(a-b)^2}{ab}\right][(1-r)^2 - \delta], \end{aligned} \tag{C7}$$

where $a = \sqrt{\delta}$ and $b = \sqrt{4r+\delta}$. Its easy to see that in the limit $r \to 0$, $a \to b$ and $\delta = u(2-u)$. This makes $\Omega^2/\tilde{\Delta}_Z^2 = (1-u)^2$ or $\Omega = \Delta_Z$, which is the bare Larmor frequency. In the opposite limit of $r \to \infty$, we find two roots: $\delta = r^2u$ and $\delta = r^2u/2$. These give $\Omega^2 = \Delta_R^2(1-u)$ or $\Delta_R^2(1-u/2)$, which are the frequencies of the two spin-chiral modes in the absence of the magnetic field.

Equation (9) corresponds to the strong-field limit and is derived assuming that $r \ll u < 1$. We skip this derivation as it is a brute force expansion in r^2, which is lengthy but completely straightforward.

In the moderate-field limit, where $r \approx 1$, we relabel $r = 1 - \varepsilon$ with $0 < \varepsilon \ll 1$ and look for a solution in the region $\delta \ll \varepsilon^2$. In this limit, the quantities X and Y reduce to

$$\begin{aligned} X &= \frac{1}{2} + \frac{3\varepsilon^2}{4\sqrt{\delta}}, \\ Y &= \frac{\varepsilon^2}{4\sqrt{\delta}}. \end{aligned} \tag{C8}$$

This yields

$$\delta = \frac{\varepsilon^4}{4}\frac{u^2(1-3u/4)^2}{(1-u)^2(1-u/2)^2}, \tag{C9}$$

which reproduces Eq. (10).

In the weak-coupling case ($u \ll 1$), one can identify one more interval: $u \ll r < 1$. There, we find that $\delta = u^2(1-r)^4/r$. This makes the frequency $\Omega^2 \approx \tilde{\Delta}_Z(1-r)[1 - \frac{u^2}{2}\frac{(1-r)^2}{r}]$, which reproduces Eq. (11).

APPENDIX D: COLLECTIVE MODES FROM THE QUANTUM KINETIC EQUATION

The quantum kinetic equation for a Fermi liquid (FL) subject to a spatially uniform external field and in the collisionless regime reads

$$i\frac{\partial \delta\hat{n}_{\vec{k}}}{\partial t} = [\delta\hat{\varepsilon}_{\vec{k}}, \hat{n}_{\vec{k}}], \tag{D1}$$

where

$$\delta\hat{\varepsilon}_{\vec{k}} = \frac{\vec{s}_{\vec{k}}\cdot\vec{\sigma}}{2} + \int_{\vec{k}'} \mathrm{Tr}'[\hat{F}_{\vec{k}\vec{k}'}\delta\hat{n}'_{\vec{k}}] \tag{D2}$$

is a variation of the quasiparticle energy, $\int_{\vec{k}'} \equiv \int \frac{d^2k'}{(2\pi)^2} = \nu_{2D}\int d\varepsilon \int \frac{d\theta}{2\pi}$, $F_{\vec{k}\vec{k}'} = F^a(\theta - \theta')\vec{\sigma}\cdot\vec{\sigma}'$ is the antisymmetric part of an SU(2)-invariant Landau interaction function, θ and θ' are the angle subtended by $\vec{k}$ and $\vec{k}'$, correspondingly, and $\vec{s}_{\vec{k}}$ parametrizes the spin-orbit and Zeeman terms of the Hamiltonian. For RSOC, $\vec{s}_{\vec{k}} = \Delta_R(\sin\theta, -\cos\theta, 0)$; for purely Zeeman coupling, $\vec{s}_{\vec{k}} = (-\tilde{\Delta}_Z, 0, 0)$; etc. The electron distribution function can be written as

$$\hat{n}_{\vec{k}} = \frac{\vec{s}_{\vec{k}}\cdot\vec{\sigma}}{2}\frac{\partial n_0}{\partial\varepsilon} + \delta\hat{n}_{\vec{k}}, \tag{D3}$$

where n_0 is the equilibrium distribution function in the absence of both SOC and magnetic field, and $\delta\hat{n}_{\vec{k}}$ is the nonequilibrium part. The nonequilibrium part of the magnetization is given by

$$\vec{M} = -\frac{g\mu_B}{2}\int_{\vec{k}} \mathrm{Tr}[\vec{\sigma}\,\delta\hat{n}_{\vec{k}}]. \tag{D4}$$

The nonequilibrium part of the distribution function can be expanded either over standard or rotated Pauli matrices [4]. In the first way, $\delta\hat{n}_{\vec{k}} = \vec{N}(\theta)\cdot\vec{\sigma}\,\frac{\partial n_0}{\partial\varepsilon}$ such that $M_i = g\mu_B\nu_{2D}\int_\theta N_i(\theta)$, with $i \in (1,2,3)$ and $\int_\theta \equiv \int_0^{2\pi} d\theta_k/(2\pi)$. The kinetic equation reads

$$\dot{\vec{N}}(\theta) = -\vec{N}(\theta)\times\vec{s}_\theta - \int_{\theta'} F^a(\theta-\theta')\vec{N}(\theta')\times\vec{s}_\theta, \tag{D5}$$

where $\vec{s}_\theta \equiv \vec{s}_{\vec{k}}$ at $k = k_F$. The time dependence of $\vec{N}$ is not explicitly specified. Equation (D5) can be solved by decomposing $\vec{N}$ and F^a into angular harmonics. Note that M_i is given by the zeroth harmonic of N_i.

As a demonstration, we solve Eq. (D5) for the case of RSOC in the s-wave approximation for $F^a(\theta-\theta') = F_0^a$. Equation (D5) is then simplified to

$$\dot{\vec{N}}(\theta) = -\vec{N}(\theta)\times\vec{s}_\theta - F_0^a\vec{M}\times\vec{s}_\theta. \tag{D6}$$

Note that $\vec{s}_\theta\cdot\dot{\vec{N}}(\theta) = 0$ suggesting that $\vec{s}_\theta\cdot\vec{N}(\theta) =$ constant, which can be set to zero. Integrating Eq. (D6) over θ and noticing that $\int_\theta \vec{s}_\theta = 0$ for RSOC, we get

$$\dot{\vec{M}} = -\int_\theta \vec{N}(\theta)\times\vec{s}_\theta. \tag{D7}$$

Differentiating Eq. (D7) over time again and using Eq. (D6) for $\dot{\vec{N}}(\theta)$ with $\vec{s}_\theta\cdot\vec{N}(\theta) = 0$, we obtain

$$\ddot{\vec{M}} = -\big(1+F_0^a\big)\Delta_R^2\vec{M} + F_0^a\int_\theta \vec{s}_\theta(\vec{s}_\theta\cdot\vec{M}). \tag{D8}$$

This yields

$$\ddot{M}_{1,2} = -\left(1+\frac{F_0^a}{2}\right)\Delta_R^2 M_{1,2}, \quad \ddot{M}_3 = -\big(1+F_0^a\big)\Delta_R^2 M_3, \tag{D9}$$

which coincides with the $q = 0$ limit of the hydrodynamic equations derived in Ref. [22].

For the field-only case, when $\vec{s}_\theta \equiv (-\tilde{\Delta}_Z,0,0)$ is isotropic in the momentum space, we obtain the familiar Bloch equation by integrating Eq. (D5) over the angle [47]

$$\dot{\vec{M}} = \big(1+F_0^a\big)\tilde{\Delta}_Z\vec{M}\times\hat{x}_1 = g\mu_B\vec{M}\times\vec{B}. \tag{D10}$$

Equivalence of the RPA and FL approaches in the s-wave approximation

The results discussed thus far were presented in with a different choice of basis [4,22] and reproduced in Ref. [23] within the RPA approximation. We now wish to reproduce the RPA result for the case of RSOC in the presence of the magnetic field using the quantum kinetic equation. It is convenient to work in the basis introduced by Ref. [4]. In this basis we write

$$\delta\hat{n} = N_i(\theta)\hat{\tau}_i\frac{\partial n_0}{\partial\varepsilon},$$
$$\hat{\tau}_1 = \hat{\sigma}_3,\ \hat{\tau}_2 = \cos\theta\hat{\sigma}_1 + \sin\theta\hat{\sigma}_2,\ \hat{\tau}_3 = \sin\theta\hat{\sigma}_1 - \cos\theta\hat{\sigma}_2. \tag{D11}$$

Expanding $N_i(\theta)$ into angular harmonics as

$$N_i(\theta) = \sum_m N_i^{(m)}\cos m\theta + \bar{N}_i^{(m)}\sin m\theta, \tag{D12}$$

and using Eq. (D4), we obtain for the magnetization components

$$\begin{aligned} M_1 &= g\mu_B\big(N_2^{(1)} + \bar{N}_3^{(1)}\big),\\ M_2 &= g\mu_B\big(\bar{N}_2^{(1)} - N_3^{(1)}\big),\\ M_3 &= g\mu_B N_1^{(0)}. \end{aligned} \tag{D13}$$

The case of RSOC only can be solved exactly for an arbitrary form of the Landau interaction function in the spin channel, $F^a(\theta-\theta')$, because equations for harmonics of $\vec{N}$ decouple in this case [4]. However, harmonics do not decouple in the presence of the field for an arbitrary Landau function, and thus an exact solution is not possible. To proceed further, we adopt the s-wave approximation, $F_0^a(\theta-\theta') = F_0^a$. In this case, the kinetic equation [Eq. (D1)] can be written as

$$\begin{aligned} \dot{N}_1(\theta) + \tilde{\Delta}_z[N_2(\theta)\sin\theta - N_3(\theta)\cos\theta] - \Delta_R N_2(\theta) &= \tilde{F}[\Delta_R(M_2\sin\theta + M_1\cos\theta) - \tilde{\Delta}_z M_2],\\ \dot{N}_2(\theta) - \tilde{\Delta}_z N_1(\theta)\sin\theta + \Delta_R N_1(\theta) &= \tilde{F}(\tilde{\Delta}_z\sin\theta - \Delta_R)M_3,\\ \dot{N}_3 + \tilde{\Delta}_z N_1(\theta)\cos\theta &= -\tilde{F}\tilde{\Delta}_z\cos\theta M_3, \end{aligned} \tag{D14}$$

where $\tilde{F} \equiv F_0^a/g\mu_B\nu_{2D}$. After a Fourier transform in time, we obtain for those harmonics of N that are relevant for magnetization

$$\begin{aligned} N_1^0 &= \frac{\tilde{F}}{2W^2\tilde{\Delta}_z f}\big[i\Omega\big\{W^2(1-f) + 2\tilde{\Delta}_z^2\big\}M_2 - 2\tilde{\Delta}_z\{(\Omega^2 + W^2 f)M_3\}\big],\\ N_2^1 &= \frac{\tilde{F}}{8\tilde{\Delta}_z^2\Delta_R^2}\big[2W^2\Delta_R^2(f-1) - \big\{W^4(f-1) + 2\tilde{\Delta}_z^2\Delta_R^2\big\}\big]M_1,\\ \bar{N}_2^1 &= \frac{\tilde{F}}{8\tilde{\Delta}_z^2\Delta_R^2 f}\big[\big\{2(1-f)\big[2\tilde{\Delta}_z^2\Delta_R^2 - W^2\big(\tilde{\Delta}_z^2 + \Delta_R^2\big)\big] - \big[2\tilde{\Delta}_z^2\Delta_R^2 f + W^4(f-1)\big]\big\}M_2\\ &\quad + 2i\Omega(1-f)\big\{W^2\tilde{\Delta}_z - 2\tilde{\Delta}_z\Delta_R^2\big\}M_3\big], \end{aligned}$$

$$N_3^1 = \frac{\tilde{F}}{8\tilde{\Delta}_z^2\Delta_R^2}\left[\left\{2W^2\tilde{\Delta}_z^2(1-f)+\left[2\tilde{\Delta}_z^2\Delta_R^2+W^4(f-1)\right]\right\}M_2+2iW^2\Omega\tilde{\Delta}_z(f-1)M_3\right],$$
$$\bar{N}_3^1 = \frac{\tilde{F}}{8\tilde{\Delta}_z^2\Delta_R^2}\left[2\tilde{\Delta}_z^2\Delta_R^2+W^4(f-1)\right]M_1, \tag{D15}$$

where f and W are given by Eqs. (C2) and (C3), correspondingly. Combining the left-hand sides of the equations above into components of $\vec{M}$, we obtain the eigenmode equation

$$\begin{pmatrix} 1-\frac{F_0^a}{2\nu_{2D}}\Pi_{11}^0(\Omega) & 0 & 0 \\ 0 & 1-\frac{F_0^a}{2\nu_{2D}}\Pi_{22}^0(\Omega) & -\frac{F_0^a}{2\nu_{2D}}\Pi_{23}^0(\Omega) \\ 0 & -\frac{F_0^a}{2\nu_{2D}}\Pi_{32}^0(\Omega) & 1-\frac{F_0^a}{2\nu_{2D}}\Pi_{33}^0(\Omega) \end{pmatrix}\begin{pmatrix} M_1 \\ M_2 \\ M_3 \end{pmatrix} = 0, \tag{D16}$$

where $\Pi_{ij}^0(\Omega)$ are the same as in Eq. (7). These are the same eigenmode equations as given by RPA, $\det[1+\frac{U}{2}\Pi]=0$, upon replacing $F_0^a \to -\nu_{2D}U$.

[1] H. L. Stormer, Z. Schlesinger, A. Chang, D. C. Tsui, A. C. Gossard, and W. Wiegmann, Energy Structure and Quantized Hall Effect of Two-Dimensional Holes, Phys. Rev. Lett. **51**, 126 (1983).

[2] D. Stein, K. v. Klitzing, and G. Weimann, Electron Spin Resonance on GaAs/Al_xGa_{1-x}As Heterostructures, Phys. Rev. Lett. **51**, 130 (1983).

[3] Z. Wilamowski, H. Malissa, F. Schäffler, and W. Jantsch, *g*-Factor Tuning and Manipulation of Spins by an Electric Current, Phys. Rev. Lett. **98**, 187203 (2007).

[4] A. Shekhter, M. Khodas, and A. M. Finkelstein, Chiral spin resonance and spin-Hall conductivity in the presence of the electron-electron interactions, Phys. Rev. B **71**, 165329 (2005).

[5] Z. Wilamowski, W. Ungier, and W. Jantsch, Electron spin resonance in a two-dimensional electron gas induced by current or by electric field, Phys. Rev. B **78**, 174423 (2008).

[6] W. Ungier and W. Jantsch, Rashba fields in a two-dimensional electron gas at electromagnetic spin resonance, Phys. Rev. B **88**, 115406 (2013).

[7] E. I. Rashba, A method of experimental examination of possibility of introduction of universal surface recombination rate during investigation of the photoelectric processes kinetics, Sov. Phys. Solid State **2**, 1109 (1960).

[8] Yu. A. Bychkov and E. Rashba, Properties of a 2D electron gas with lifted spectral degeneracy, JETP Lett. **39**, 78 (1984); Oscillatory effects and the magnetic susceptibility of carriers in inversion layers, J. Phys. C **17**, 6039 (1984).

[9] G. Dresselhaus, Spin-orbit coupling effects in zinc blende structures, Phys. Rev. **100**, 580 (1955).

[10] M. I. Dyakonov and V. Yu. Kachorovskii, Spin relaxation of two-dimensional electrons in noncentrosymmetric semiconductors, Sov. Phys. Semicond. **20**, 110 (1986).

[11] R. Winkler, *Spin-Orbit Coupling Effects in Two-Dimensional Electron and Hole Systems* (Springer, Berlin, 2003).

[12] E. I. Rashba and V. I. Sheka, Electric-dipole spin resonance, in *Landau Level Spectroscopy*, edited by G. Landwehr and E. I. Rashba (North-Holland, Amsterdam, 1991), p. 131.

[13] E. I. Rashba and Al. L. Efros, Efficient electron spin manipulation in a quantum well by an in-plane electric field, Appl. Phys. Lett. **83**, 5295 (2003).

[14] Al. L. Efros and E. I. Rashba, Theory of electric dipole spin resonance in a parabolic quantum well, Phys. Rev. B **73**, 165325 (2006).

[15] M. Duckheim and D. Loss, Electric-dipole-induced spin resonance in disordered semiconductors, Nat. Phys. **2**, 195 (2006).

[16] M. Schulte, J. G. S. Lok, G. Denninger, and W. Dietsche, Electron Spin Resonance on a Two-Dimensional Electron Gas in a Single AlAs Quantum Well, Phys. Rev. Lett. **94**, 137601 (2005).

[17] V. P. Silin, Oscillations of a Fermi liquid in a magnetic field, Sov. Phys. JETP **6**, 945 (1958).

[18] A. J. Leggett, Spin diffusion and spin echoes in liquid ^{3}He at low temperature, J. Phys. C **3**, 448 (1970).

[19] Y. Yafet, *g*-factors and spin-lattice relaxation, in *Solid State Physics*, Vol. 14, edited by F. Seitz and D. Turnbull (Academic, New York, 1963), p. 92.

[20] S. S. Krishtopenko, V. I. Gavrilenko, and M. Goiran, Spin-wave excitations and electron spin resonance in symmetric and asymmetric narrow-gap quantum wells, Phys. Rev. B **87**, 155113 (2013); **88**, 039907(E) (2013).

[21] R. Glenn, O. A. Starykh, and M. E. Raikh, Interplay of spin-orbit coupling and Zeeman splitting in the absorption line shape of fermions in two dimensions, Phys. Rev. B **86**, 024423 (2012).

[22] A. Ashrafi and D. L. Maslov, Chiral Spin Waves in Fermi Liquids with Spin-Orbit Coupling, Phys. Rev. Lett. **109**, 227201 (2012).

[23] S. Maiti, V. A. Zyuzin, and D. L. Maslov, Collective modes in two- and three-dimensional electron systems with Rashba spin-orbit coupling, Phys. Rev. B **91**, 035106 (2015).

[24] M. I. D'yakonov and V. I. Perel', Spin relaxation of conduction electrons in noncentrosymmetric semiconductors, Sov. Phys. Solid State **13**, 3023 (1972).

[25] M. M. Glazov and E. L. Ivchenko, Effect of electron-electron interaction on spin relaxation of charge carriers in semiconductors, JETP **99**, 1279 (2004).

[26] A. Punnoose and A. M. Finkel'stein, Spin Relaxation in the Presence of Electron-Electron Interactions, Phys. Rev. Lett. **96**, 057202 (2006).

[27] S. D. Ganichev and L. E. Golub, Interplay of Rashba/Dresselhaus spin splittings probed by photogalvanic spectroscopy: A review, Phys. Status Solidi B **251**, 1801 (2014).

[28] A. E. Meyerovich and K. A. Musaelian, Zero-temperature attenuation and transverse spin dynamics in Fermi liquids. I. Generalized Landau theory, J. Low Temp. Phys. **89**, 781 (1992); Zero-temperature attenuation and transverse spin dynamics in Fermi liquids. II. Dilute Fermi system, **94**, 249 (1994); Zero-temperature attenuation and transverse spin dynamics in Fermi liquids. III. Low spin polarizations, **95**, 789 (1994).

[29] A. Ashrafi, E. I. Rashba, and D. L. Maslov, Theory of a chiral Fermi liquid: General formalism, Phys. Rev. B **88**, 075115 (2013).

[30] In the s-wave approximation, α is not renormalized by the electron-electron interaction. In a more general treatment, α should be understood as a renormalized value of the Rashba parameter [4,31,32].

[31] G.-H. Chen and M. E. Raikh, Exchange-induced enhancement of spin-orbit coupling in two-dimensional electronic systems, Phys. Rev. B **60**, 4826 (1999).

[32] D. S. Saraga and D. Loss, Fermi liquid parameters in two dimensions with spin-orbit interaction, Phys. Rev. B **72**, 195319 (2005).

[33] B. M. Norman, C. J. Trowbridge, J. Stephens, A. C. Gossard, D. D. Awschalom, and V. Sih, Mapping spin-orbit splitting in strained (In,Ga)As epilayers, Phys. Rev. B **82**, 081304(R) (2010).

[34] B. M. Norman, C. J. Trowbridge, D. D. Awschalom, and V. Sih, Current-Induced Spin Polarization in Anisotropic Spin-Orbit Fields, Phys. Rev. Lett. **112**, 056601 (2014).

[35] M. Luengo-Kovac, M. Macmahon, S. Huang, R. S. Goldman, and V. Sih, g-factor modification in a bulk InGaAs epilayer by an in-plane electric field, Phys. Rev. B **91**, 201110(R) (2015).

[36] Z. Wilamowski, W. Jantsch, H. Malissa, and U. Rössler, Evidence and evaluation of the Bychkov-Rashba effect in SiGe/Si/SiGe quantum wells, Phys. Rev. B **66**, 195315 (2002).

[37] Y. Kozuka, S. Teraoka, J. Falson, A. Oiwa, A. Tsukazaki, S. Tarucha, and M. Kawasaki, Rashba spin-orbit interaction in a $Mg_xZn_{1x}O$/ZnO two-dimensional electron gas studied by electrically detected electron spin resonance, Phys. Rev. B **87**, 205411 (2013).

[38] F. Baboux, F. Perez, C. A. Ullrich, I. D'Amico, G. Karczewski, and T. Wojtowicz, Coulomb-driven organization and enhancement of spin-orbit fields in collective spin excitations, Phys. Rev. B **87**, 121303(R) (2013).

[39] F. Baboux, F. Perez, C. A. Ullrich, I. D'Amico, J. Gómez, and M. Bernard, Giant Collective Spin-Orbit Field in a Quantum Well: Fine Structure of Spin Plasmons, Phys. Rev. Lett. **109**, 166401 (2012).

[40] L. Meier, G. Salis, I. Shorubalko, E. Gini, S. Schoen, and K. Ensslin, Measurement of Rashba and Dresselhaus spin-orbit magnetic fields, Nat. Phys. **3**, 650 (2007).

[41] J. B. Miller, D. M. Zumbühl, C. M. Marcus, Y. B. Lyanda-Geller, D. Goldhaber-Gordon, K. Campman, and A. C. Gossard, Gate-Controlled Spin-Orbit Quantum Interference Effects in Lateral Transport, Phys. Rev. Lett. **90**, 076807 (2003).

[42] Y. H. Park, H.-J. Kim, J. Chang, S. H. Han, J. Eom, H.-J. Choi, and H. C. Koo, Separation of Rashba and Dresselhaus spin-orbit interactions using crystal direction dependent transport measurements, Appl. Phys. Lett. **103**, 252407 (2013).

[43] T. P. Smith III and F. F. Fang, g factor of electrons in an InAs quantum well, Phys. Rev. B **35**, 7729 (1987).

[44] J. P. Heida, B. J. van Wees, J. J. Kuipers, T. M. Klapwijk, and G. Borghs, Spin-orbit interaction in a two-dimensional electron gas in a InAs/AlSb quantum well with gate-controlled electron density, Phys. Rev. B **57**, 11911 (1998).

[45] J. Nitta, T. Akazaki, H. Takayanagi, and T. Enoki, Gate Control of Spin-Orbit Interaction in an Inverted $In_{0.53}Ga_{0.47}As/In_{0.52}Al_{0.48}As$ Heterostructure, Phys. Rev. Lett. **78**, 1335 (1997).

[46] Y. Wiemann, J. Simmendinger, C. Clauss, L. Bogani, D. Bothner, D. Koelle, R. Kleiner, M. Dressel, and M. Scheffler, Observing electron spin resonance between 0.1 and 67 GHz at temperatures between 50 mK and 300 K using broadband metallic coplanar waveguides, Appl. Phys. Lett. **106**, 193505 (2015).

[47] E. M. Lifshitz and L. P. Pitaevskii, *Statistical Physics Part II* (Pergamon Press, New York, 1980).